Accepted manuscript doi:
10.1680/jgele.19.00040

Submitted: 17 March 2019

Published online in 'accepted manuscript' format: 03 July 2019

Manuscript title: The effect of negative excess pore-water pressure on the stability of excavated slopes

Authors: M. Ghadrdan*, T. Shaghaghi* and A. Tolooiyan†

Affiliations: *Geotechnical and Hydrogeological Engineering Research Group (GHERG), Federation University Australia, Churchill, VIC 3842, Australia and †School of Engineering, College of Sciences and Engineering, University of Tasmania, Hobart, TAS 7001, Australia

Corresponding author: Ali Tolooiyan, School of Engineering, College of Sciences and Engineering, University of Tasmania, Hobart, TAS 7001, Australia. Tel.: +61 3 6226 2429.

E-mail: ali.tolooiyan@utas.edu.au, tolooiyan@gmail.com

Accepted manuscript doi:
10.1680/jgele.19.00040

Abstract

The generation of Negative Excess Pore-Water Pressure (NEPWP) due to the excavation of saturated soils under undrained conditions and the following dissipation of this phenomenon over time may result in different short- and long-term slope instability. The NEPWP generated due to excavation gradually decreases towards equilibrium or in some cases steady seepage. Hence, total pore-water pressures immediately after the excavation are lower than the ultimate equilibrium values, leading to the reduction of the average effective stresses in the slope and subsequently threatening the stability in the long term. In this research, the stability of three benchmark civil and mining excavations has been studied, considering the effects of generation and dissipation of NEPWP. A series of numerical simulations are conducted to determine the role of in-situ stresses and time in NEPWP dissipation as well as the consequent effects on the stability of the excavated slopes. To conduct a realistic time-dependent transient analysis, a fully-coupled hydro-geomechanical formulation has been employed. Results show that in general, higher removal of stress levels leads to higher NEPWP generation and higher factor of safety values in the short term. Thereafter, the dissipation of NEPWP threatens the long-term stability of the excavation.

Keywords: excavation; pore pressures; time dependency

Accepted manuscript doi:
10.1680/jgele.19.00040

1. Introduction

Generation of either pore-water pressures or pore-water tension plays a key role in the stability of slopes (Ridley et al., 2004, Conte and Troncone, 2012, Zhang et al., 2011, Lollino et al., 2011, Yu-qi et al., 2005, Vaughan and Walbancke, 1973, Eigenbrod, 1975, Cai and Ugai, 2004). When saturated soil is under compression in undrained condition, the system resists being compressed by generating excess pore-water pressure which leads to a reduction of effective stresses. By dissipating the developed excess pore-water pressure over time, the effective stress and shear strength increase gradually (Griffiths and Li, 1993, Bishop and Bjerrum, 1960, Day et al., 2001). This phenomenon can cause significant problems for the short-term stability of geotechnical projects.

By removing a mass of material through excavation in undrained conditions, the reduction of total stresses leads to a pore-water pressure reaction while the pore-water pressure becomes depressed to compensate such a reduction. This phenomenon starts with the generation of excess pore-water tension or NEPWP in beneath and adjacent to the removed soil mass (Potts et al., 2009). By assuming unloading in a fully-saturated and under undrained conditions with linear elastic behaviour, the reduction in mean stress levels due to the unloading is equal to the generation of NEPWP (L'Heureux et al., 2009, Bishop and Bjerrum, 1960, Eigenbrod, 1975, Bishop, 1953, Griffiths and Li, 1993, Bishop et al., 1975, Wang et al., 2003). The induced NEPWP subsequently increases the effective stresses and the shear strength of the materials.

By the passage of time, the generated NEPWP dissipates, accompanied by swelling of the pit floor until steady-state conditions are reached (Eigenbrod, 1975). Since the change of shear strength is associated with the development and dissipation of NEPWP, the shear strength of the influenced zone will decrease gradually due to the dissipation of NEPWP and increase of total pore-water pressure (Bishop and Bjerrum, 1960). It follows that the stability of the formed slope may vary after excavation until reaching steady-state conditions at the rate at which swelling occurs (James, 1970b, Griffiths and Li, 1993, Vaughan and Walbancke, 1973). From the literature it is a well-known fact that several slopes have failed after the equilibration of the generated NEPWP (Vaughan and Walbancke, 1973, Hughes et al., 2007, Potts et al., 2009, Kovacevic et al., 2011, Kovacevic et al., 2004, Lollino et al., 2011).

The redistribution of pore-water pressure caused due to excavation could be a function of several factors such as the excavation geometry, in-situ stresses, materials' permeability, hydraulic boundary conditions, stratigraphy, seasonal variation and soils' microstructures (De la Fuente et al., 2015, Lollino et al., 2011, Leroueil, 2001, L'Heureux et al., 2009, Rankka, 1994, Lafleur et al., 1988, Skempton, 1984).

Accepted manuscript doi:
10.1680/jgele.19.00040

Similar to the dissipation rate of pore-water pressure, in coarse-grained soils such as gravel and sand, NEPWP dissipates easily due to high permeability. However, in fine-grained soils such as clay and silt, the dissipation of NEPWP takes longer. During and after excavation, the stress redistribution due to dewatering, unloading and swelling can initiate new cracks and fissures, or open the existing ones. Such discontinuities act as seepage paths which increase the permeability of the soil mass and subsequently affect the rate of NEPWP generation and dissipation (Vaughan and Walbancke, 2009, Eigenbrod, 1975, James, 1970a, Cotecchia et al., 2015, Pedone et al., 2016, Vaughan and Walbancke, 1973, Griffiths and Li, 1993). Also, the dewatering and desaturating of soil may result in drying cracking (Hueckel et al., 2013, Peron et al., 2009). The suction development in drying cracking zones is a multi-physical process which depends on several factors such as vapor flux, air and water flow at the pore vessels and pore size distribution (Hueckel et al., 2013, Cafaro and Cotecchia, 2015). Furthermore, several studies (Hueckel et al., 2013, Peron et al., 2009, Cotecchia and Vitone, 2011, Cotecchia et al., 2015) have been conducted to investigate the effect of fissuring on the hydromechanical behaviour of soil at micro scales and it is widely accepted that the pore-water pressure and suction generation is strongly dependent on soil microstructure.

Although the phenomenon of generation of NEPWP due to excavation has been investigated to some extent, the dissipation of NEPWP and its effect on the slope stability are rarely studied. In this study, for a greater understanding of the effect of this phenomenon on the stability of slopes, three different practical benchmarks with different values of the earth coefficient (k_0) are investigated through a fully-coupled flow-deformation analysis by Finite Element (FE) method. It should be noted that the development of cracks and fissures is beyond the scope of this study, and the possible variation of permeability subsequent to cracking is not considered in the presented analyses.

2. Methodology

When excavating a saturated soil and dewatering a pit, the removed vertical and horizontal stresses are as follows:

$$\sigma_v = \gamma_t h \qquad 1.$$

$$\sigma_h = K_0 \sigma_v^{'} + u = h\left[K_0\left(\gamma_t - \gamma_w\right) + \gamma_w\right] \qquad 2.$$

Accepted manuscript doi:
10.1680/jgele.19.00040

By removing the stresses, the change in pore pressure immediately after unloading and over time can be defined as follows (Vaughan and Walbancke, 1973, Skempton, 1954, Eigenbrod, 1975):

$$\Delta u = \Delta\sigma_3 + A\left(\Delta\sigma_1 - \Delta\sigma_3\right) \qquad 3.$$

$$u_0 = u - \Delta u = \gamma_w h - \Delta u \qquad 4.$$

$$\Delta u_e = u_0 - u_t \qquad 5.$$

The dissipation of generated NEPWP can be considered as a reverse of the consolidation process which follows the conventional Terzaghi theory for consolidation (Yu-qi et al., 2005, Eigenbrod, 1975, Vaughan and Walbancke, 1973, Di Francesco, 2011) (see Eq. 6).

$$c_h \frac{\partial^2 u}{\partial x^2} + c_h \frac{\partial^2 u}{\partial y^2} + c_v \frac{\partial^2 u}{\partial z^2} = \frac{\partial u}{\partial t} \qquad 6.$$

To evaluate the stability of slopes, there are several methods of analysis, of which the Limit Equilibrium Method (LEM) and Finite Element Method (FEM) are the two most commonly used (Abramson et al., 2002, Eberhardt, 2003, Griffiths and Lane, 1999, Aryal, 2006, Hammah et al., 2010, Huang and Jia, 2009, Matsui and San, 1992, Ugai and Leshchinsky, 1995, Dawson et al., 1999, Liu et al., 2015, Tolooiyan et al., 2009, Vekli et al., 2012, Raghuvanshi, 2017, Krahn, 2003).

In this study, to observe the effect of generation and dissipation of NEPWP after excavation on the stability of the formed slopes, the Shear Strength Reduction Finite Element Method (SSR-FEM) (Dyson and Tolooiyan, 2018, Dyson and Tolooiyan, 2019, Aryal, 2006, Griffiths and Lane, 1999) is applied in *PLAXIS 2D* (PLAXIS, 2018) and *PLAXIS 3D* (PLAXIS, 2017).

3. Numerical modelling

Three different benchmark analyses are conducted in this study (Figures 1-3). Benchmark 1 is a Two-Dimensional (2D) simulation of a vertical urban excavation which is carried out in three stages (each 5m deep) over 3 days. As a common urban excavation project, the vertical wall is reinforced for the safety of the project. Hence, a 21m long concrete diaphragm wall with a thickness of 0.35m is installed in the ground. Also, the wall

Accepted manuscript doi:
10.1680/jgele.19.00040

is ditched to the surrounding soil with two rows of anchors with a total length of 18.8m (anchor rod and grout body) and inclination of 32 degrees (see Figure 1).

Benchmark 2 is a 2D excavation of an open-pit mine where 70m of the material is excavated during 180 days (see Figure 2).

Benchmark 3 is a Three-Dimensional (3D) excavation of an open-pit mine where 80m of the materials is excavated over 365 days (see Figure 3).

For the soil materials constitutive modelling, the Hardening Soil (HS) model (Schanz et al., 1999) is employed and the model's parameters are presented in Table 1. Also, for benchmark 1, the properties of structural elements are presented in Table 2. Different values of K_0 are assumed to study the effect of in-situ stresses on the generation and dissipation of NEPWP. For the 2D FEM models, the element type is 15-node triangle and for the 3D model, is 10-node tetrahedral.

To satisfy suitable boundary conditions, the geometries are extended sufficiently vertically from the ground surface, and horizontally from the toe and the crest of slopes. The vertical boundaries of the model are horizontally fixed while the bottom boundary is fully fixed (horizontally and vertically). In addition, the hydrostatic boundary conditions for analysis is defined as: 1) seepage through the vertical boundaries, 2) no seepage through the bottom of the model, and 3) groundwater table is set at the ground level.

4. Analysis results

By conducting a series of fully-coupled analyses of three different benchmarks with different in-situ stress levels, the generation and dissipation of NEPWP are investigated. It is noted that the distribution of generated NEPWP is not uniform and due to the major influence of the stress level removal, the maximum values have been generated in the zones below the foundation pits of the three benchmarks (see Figures 4-8).

It can be seen that the greater K_0 creates greater NEPWP levels that are due to more removal of stress levels in the excavation process and the magnitude of generated NEPWP can be more significant in deep excavations.

Figures 9-11 presents the dissipation trends of the generated NEPWP below the foundation pits for different situations. The highlighted rectangles show the time period in which the most significant reduction of maximum NEPWP occurred. This period is approximately 20-30% of the total time required for reaching steady-state conditions and water pressure equilibrium.

The distribution and variation of the generated NEPWP depend on several factors such as removal stress levels, excavation time, and drainage conditions. Furthermore, the maximum value of NEPWP is not necessarily

generated in the potential slip surface. Hence, the aforementioned time cannot be a critical time for evaluating the stability of slopes. Therefore, the effective time which equilibrates the pore-water pressure within the potential slip surface should be investigated.

By conducting a back analysis, the points located at the maximum depth of the potential slip surface are chosen as reference points for three benchmarks (see Figure12). The effective time for dissipation of NEPWP in the slip surface can be found out by analysing the changes of total pore pressure trends at the reference points over time. The relationship between the total pore pressure at the reference point and time is generated and can be written in the form of the one-site binding equation (see Eq. 10).

$$P_{active} = B\frac{t}{C+t} + D\times t + E \qquad 10.$$

By equating the derived one-site binding equation to zero and solving the obtained quadratic equation, the effective time (see Eq. 11) for analysing the stability of the slopes can be derived as the time at which the change in the slope of total pore pressure versus time at the reference points becomes negligible. Table 3 presents the required time for the dissipation of generated NEPWP at the potential slip surfaces. As shown in this table, the dissipation of generated NEPWP takes longer in those cases at which K_0 values and stress level removals are higher.

$$t_e = \frac{-2C \pm \sqrt{(2C)^2 - 4\left(C^2 + \frac{B\times C}{D}\right)}}{2} \qquad 11.$$

Figures 4 (c), 5 (c), and 8 present the distribution of NEPWP for the three benchmarks just after excavation (at $0.0t_e$), while K_0 =2. Also, Figures 13-16 present the distribution of NEPWP at $0.5t_e$ and $1.0t_e$ after excavation. By comparing the distribution of NEPWP, it can be seen that significant portion of the generated NEPWP dissipates before $0.5t_e$ is reached.

Since the dissipation of NEPWP occurs over time, a time-dependent slope stability study is conducted. Figures 17-19 present the evolution of FoS versus the normalised effective time (t/t_e).

Accepted manuscript doi:
10.1680/jgele.19.00040

The in-situ stress levels play a key role in the stability of the slopes formed by excavation in a saturated soil which is under a slow rate of drainage (due to low permeability or insufficient time). From Figures17-19, it is observed that the major reduction in FoS occurred during the time span from the excavation to the normalised effective time (t/t_e) equal to 0.2 - 0.3. Over this period, the generated NEPWP due to the excavation dissipates at a high rate while the effective stresses decrease simultaneously. For the given benchmark analyses, the reduction of FoS for the time span before and after t/t_e=0.3 are presented in Table 4.

Table 4 shows that the greater K_0 values result in greater reduction of FoS as the consequence of NEPWP dissipation. This is due to the fact that the higher K_0 generates higher in-situ stress levels. Greater stress level removal due to excavation imposes more generation of NEPWP levels and higher FoS values in the short term. After the dissipation of the generated NEPWP, the cases with higher stress level removal, show the higher reduction of FoS in the long term.

5. Conclusion

Ground excavation causes a decrease in mean stress and an increase in shear stress. When the removal of materials is under undrained condition with insufficient time or low permeability, there will be an associated generation of NEPWP in the soil mass. Generally, the higher K_0 values and the greater depth of excavation, the greater effective stress removal, and consequently greater NEPWP generation.

The process of equalisation of the generated NEPWP and the resultant reduction of the effective stresses in the slope is a significant factor which affects the stability of a slope over time. The results presented in this paper show that the rate of equilibration of generated NEPWP after excavation is rapid firstly and after some time, the trend continues slightly. Reaching full pore pressure equilibration may take a long time depending on factors such as geometry and drainage conditions. However, in general, roughly 20-30% of this time is equal to the effective time at which rapid reduction of NEPWP completes.

Immediately after excavation, the stability FoS values for the slopes are much higher than those calculated at the steady state conditions (very long-term) when NEPWP has dissipated. Furthermore, since, the greater K_0 and removal stress resulted in greater NEPWP, over dissipation of NEPWP, greater reduction of FoS are resulted as a function of K_0. In overall, it can be concluded that depends on several factors such as stress level removal and drainage conditions, pore-water tension equalisation can be a significant trigger of instability in excavation walls in the long term.

Accepted manuscript doi:
10.1680/jgele.19.00040

Acknowledgements

Financial support for this research has been provided by Earth Resources Regulation of the Victorian State Government Department of Economic Development, Jobs, Transport and Resources. The first and second authors are funded by the GHERG LV Batter Stability Scholarship and Faculty Tuition Scholarship of Federation University Australia.

List of notations

σ_v is the removed total vertical stress

γ_t is the total unit weight of the soil

h is the depth of excavation

σ_h is the removed total horizontal stress

K_0 is the earth pressure coefficient at rest

σ_v' is the removed effective vertical stress

u is the total pore pressure

γ_w is the unit weight of water

Δu is the changes in total principal stresses due to loading

$\Delta\sigma_3$ is the changes in minimum principal stress

A is Skempton's pore pressure parameter

$\Delta\sigma_1$ is the changes in maximum principal stress

u_0 is the initial total pore pressure

u is the pore-water pressure

Δu is the changes in pore water-pressure

Δu_e is the changes in excess pore-pressure

u_t is the pore pressure at the stabilised groundwater conditions

c_h is the horizontal coefficient of consolidation

c_v is the vertical coefficient of consolidation

E_{50}^{ref} is the secant stiffness in standard drained triaxial test

E_{oed}^{ref} is the tangent stiffness for primary oedometer loading

E_{ur}^{ref} is the unloading/reloading stiffness

P_{active} is the active pressure

B is the maximum specific binding

t is the time

C is the equilibrium binding constant

D is the slope of nonspecific binding

E is the amount of nonspecific binding

t_e is the effective dissipation time

Accepted manuscript doi:
10.1680/jgele.19.00040

REFERENCES

ABRAMSON, L. W., LEE, T. S., SHARMA, S. & BOYCE, G. M. 2002. *Slope stability and stabilization methods*, John Wiley & Sons.

ARYAL, K. P. 2006. Slope stability evaluations by limit equilibrium and finite element methods.

BISHOP, A. 1953. Pore pressure changes during shear in two undisturbed clays. *Proc. 3^< rd>. ICSMFE*.

BISHOP, A. W. & BJERRUM, L. 1960. The relevance of the triaxial test to the solution of stability problems. *Norwegian Geotechnical Institute Publ*.

BISHOP, A. W., KUMAPLEY, N. & EL-RUWAYIH, A. 1975. The influence of pore-water tension on the strength of clay. *Philosophical Transactions of the Royal Society of London. Series A, Mathematical and Physical Sciences,* 278**,** 511-554.

CAFARO, F. & COTECCHIA, F. 2015. Influence of the mechanical properties of consolidated clays on their water retention curve. *Italian Geotechnical Journal,* 2**,** 13-29.

CAI, F. & UGAI, K. 2004. Numerical analysis of rainfall effects on slope stability. *International Journal of Geomechanics,* 4**,** 69-78.

CONTE, E. & TRONCONE, A. 2012. Stability analysis of infinite clayey slopes subjected to pore pressure changes. *Géotechnique,* 62**,** 87-91.

COTECCHIA, F. & VITONE, C. On the model requirements to predict the behaviour of fissured clays. Proceedings of the XV European conference on soil mechanics and geotechnical engineering, Athens, Greece, 2011. 525-530.

COTECCHIA, F., VITONE, C., SANTALOIA, F., PEDONE, G. & BOTTIGLIERI, O. 2015. Slope instability processes in intensely fissured clays: case histories in the Southern Apennines. *Landslides,* 12**,** 877-893.

DAWSON, E., ROTH, W. & DRESCHER, A. 1999. Slope stability analysis by strength reduction. *Geotechnique,* 49**,** 835-840.

DAY, R., HIGHT, D. & POTTS, D. 2001. Coupled Pore Pressure and Stability Analysis of Embankment Dam Construction. *Computational Mechanics–New Frontiers for the New Millennium.* Elsevier.

DE LA FUENTE, M., VAUNAT, J., PEDONE, G., COTECCHIA, F., SOLLECITO, F. & CASINI, F. Permeability changes induced by microfissure closure and opening in tectonized materials. Effect on slope pore pressure regime. EGU General Assembly Conference Abstracts, 2015.

DI FRANCESCO, R. 2011. Exact solutions of two-dimensional and tri-dimensional consolidation equations. *arXiv preprint arXiv:1103.6084*.

DYSON, A. P. & TOLOOIYAN, A. 2018. Optimisation of strength reduction finite element method codes for slope stability analysis. *Innovative Infrastructure Solutions,* 3**,** 1-12.

DYSON, A. P. & TOLOOIYAN, A. 2019. Prediction and classification for finite element slope stability analysis by random field comparison. *Computers and Geotechnics,* 109**,** 117-129.

EBERHARDT, E. 2003. Rock slope stability analysis-Utilization of advanced numerical techniques. *Earth and Ocean sciences at UBC*.

EIGENBROD, K. D. 1975. Analysis of the pore pressure changes following the excavation of a slope. *Canadian Geotechnical Journal,* 12**,** 429-440.

GRIFFITHS, D. & LANE, P. 1999. Slope stability analysis by finite elements. *Geotechnique,* 49**,** 387-403.

Accepted manuscript doi:
10.1680/jgele.19.00040

GRIFFITHS, D. & LI, C. 1993. Analysis of delayed failure in sloping excavations. *Journal of geotechnical engineering,* 119**,** 1360-1378.

HAMMAH, R., YACOUB, T., CORKUM, B. & CURRAN, J. 2010. A comparison of finite element slope stability analysis with conventional limit-equilibrium investigation.

HUANG, M. & JIA, C.-Q. 2009. Strength reduction FEM in stability analysis of soil slopes subjected to transient unsaturated seepage. *Computers and Geotechnics,* 36**,** 93-101.

HUECKEL, T., MIELNICZUK, B., EL YOUSSOUFI, M. S., HU, L. & LALOUI, L. Soil suction and cracking from the onset to the end of desaturation: micro-scale evidence and model. International Symposium on Computational Geomechanics COMGEO III, 2013. 371-380.

HUGHES, D., SIVAKUMAR, V., GLYNN, D. & CLARKE, G. 2007. A case study: delayed failure of a deep cutting in lodgement till. *Proceedings of the Institution of Civil Engineers-Geotechnical Engineering,* 160**,** 193-202.

JAMES, P. 1970a. *Time effects andprogressive failure in clay slopes.* PhD thesis, University of London.

JAMES, P. M. 1970b. Time effects and progressive failure in clay slopes.

KOVACEVIC, N., HIGHT, D. & POTT, D. Predicting the stand-up time of temporary London Clay slopes at Terminal 5, Heathrow Airport. Stiff Sedimentary Clays: Genesis and Engineering Behaviour: Géotechnique Symposium in Print 2007, 2011. Thomas Telford Ltd, 241-252.

KOVACEVIC, N., HIGHT, D. & POTTS, D. Temporary slope stability in London clay-Back analyses of two case histories. Advances in geotechnical engineering: The Skempton conference: Proceedings of a three day conference on advances in geotechnical engineering, organised by the Institution of Civil Engineers and held at the Royal Geographical Society, London, UK, on 29–31 March 2004, 2004. Thomas Telford Publishing, 842-855.

KRAHN, J. 2003. The 2001 RM Hardy Lecture: The limits of limit equilibrium analyses. *Canadian Geotechnical Journal,* 40**,** 643-660.

L'HEUREUX, J., LEROUEIL, S. & LAFLAMME, J. 2009. Evolution of the factor of safety following excavation in clay. *Canadian Geotechnical Journal,* 46**,** 487-493.

LAFLEUR, J., SILVESTRI, V., ASSELIN, R. & SOULIÉ, M. 1988. Behaviour of a test excavation in soft Champlain Sea clay. *Canadian Geotechnical Journal,* 25**,** 705-715.

LEROUEIL, S. 2001. Natural slopes and cuts: movement and failure mechanisms. *Géotechnique,* 51**,** 197-243.

LIU, S., SHAO, L. & LI, H. 2015. Slope stability analysis using the limit equilibrium method and two finite element methods. *Computers and Geotechnics,* 63**,** 291-298.

LOLLINO, P., SANTALOIA, F., AMOROSI, A. & COTECCHIA, F. 2011. Delayed failure of quarry slopes in stiff clays: the case of the Lucera landslide. *Géotechnique,* 61**,** 861-874.

MATSUI, T. & SAN, K.-C. 1992. Finite element slope stability analysis by shear strength reduction technique. *Soils and foundations,* 32**,** 59-70.

PEDONE, G., TSIAMPOUSI, A., COTECCHIA, F. & ZDRAVKOVIC, L. Effects of soil-vegetation-atmosphere interaction on the stability of a clay slope: a case study. E3S Web of Conferences, 2016. EDP Sciences, 15002.

PERON, H., HUECKEL, T., LALOUI, L. & HU, L. 2009. Fundamentals of desiccation cracking of fine-grained soils: experimental characterisation and mechanisms identification. *Canadian Geotechnical Journal,* 46**,** 1177-1201.

PLAXIS. 2017. *Plaxis 3D* [Online]. Delft, Netherland. Available: https://www.plaxis.com/product/plaxis-3d/ [Accessed].

PLAXIS. 2018. *Plaxis 2D* [Online]. Delft, Netherland. Available: https://www.plaxis.com/product/plaxis-2d/ [Accessed].

POTTS, D., KOVACEVIC, N. & VAUGHAN, P. 2009. Delayed collapse of cut slopes in stiff clay. *Selected papers on geotechnical engineering by PR Vaughan.* Thomas Telford Publishing.

RAGHUVANSHI, T. K. 2017. Plane failure in rock slopes–A review on stability analysis techniques. *Journal of King Saud University-Science*.

RANKKA, K. 1994. In situ stress conditions across clay slopes. A study comprising seven test sites. *CHALMERS TEKNISKA HOGSKOLA, GOTEBORG,(SWED). 1994.*

RIDLEY, A., MCGINNITY, B. & VAUGHAN, P. 2004. Role of pore water pressures in embankment stability. *Proceedings of the Institution of Civil Engineers-Geotechnical engineering,* 157**,** 193-198.

SCHANZ, T., VERMEER, P. & BONNIER, P. 1999. The hardening soil model: formulation and verification. *Beyond 2000 in computational geotechnics***,** 281-296.

SKEMPTON, A. 1954. The pore-pressure coefficients A and B. *Geotechnique,* 4**,** 143-147.

SKEMPTON, A. 1984. Slope stability of cuttings in brown London clay. *Selected Papers on Soil Mechanics.* Thomas Telford Publishing.

TOLOOIYAN, A., ABUSTAN, I., SELAMAT, M. & GHAFFARI, S. 2009. A comprehensive method for analyzing the effect of geotextile layers on embankment stability. *Geotextiles and Geomembranes,* 27**,** 399-405.

UGAI, K. & LESHCHINSKY, D. 1995. Three-dimensional limit equilibrium and finite element analyses: a comparison of results. *Soils and foundations,* 35**,** 1-7.

VAUGHAN, P. & WALBANCKE, H. 1973. Pore pressure changes and the delayed failure of cutting slopes in overconsolidated clay. *Géotechnique,* 23**,** 531-539.

VAUGHAN, P. & WALBANCKE, H. 2009. Pore pressure changes and the delayed failure of cutting slopes in overconsolidated clay. *Selected papers on geotechnical engineering by PR Vaughan.* Thomas Telford Publishing.

VEKLI, M., AYTEKIN, M., IKIZLER, S. B. & ÇALIK, Ü. 2012. Experimental and numerical investigation of slope stabilization by stone columns. *Natural hazards,* 64**,** 797-820.

WANG, Z., ZOU, W. & LI, G. 2003. Earth pressure and water pressure on retaining structure. *ROCK AND SOIL MECHANICS-WUHAN-,* 24**,** 146-150.

YU-QI, L., HONG-WEI, Y. & KANG-HE, X. 2005. On the dissipation of negative excess porewater pressure induced by excavation in soft soil. *Journal of Zhejiang University-SCIENCE A,* 6**,** 188-193.

ZHANG, L., ZHANG, J., ZHANG, L. & TANG, W. 2011. Stability analysis of rainfall-induced slope failure: a review. *Proceedings of the Institution of Civil Engineers-Geotechnical Engineering,* 164**,** 299-316.

Accepted manuscript doi:
10.1680/jgele.19.00040

Table captions

Table 1. Properties of the materials for benchmarks 1, 2 and 3

Benchmark	Benchmark 1		Benchmark 2		Benchmark 3	
Type of material	Material (I)	Material (II)	Material (III)	Material (IV)	Material (V)	Material (VI)
Dry unit weight (kN/m^3)	19	22	22	21	18	20
Saturated unit weight (kN/m^3)	22	24	23	23	20	22
E_{50}^{ref} (MPa)	40	100	300	200	100	80
E_{oed}^{ref} (MPa)	40	100	300	200	100	80
E_{ur}^{ref} (MPa)	120	300	900	600	300	240
Cohesion (kN/m^2)	20	30	70	5	140	110
Friction angle (degree)	32	25	25	33	25	20
Permeability (m/day)	0.01	0.001	0.0002	0.002	0.0001	0.0001
K_0	1, 1.5, 2	1, 1.5, 2	1, 1.5, 2	1, 1.5, 2	1, 1.5, 2	1, 1.5, 2

Table 2. Properties of the structural elements for benchmark 1

Concrete diaphragm wall			
Normal stiffness (kN/m)	Flexural rigidity (kN m^2/m)	Weight (kN/m/m)	Poission's ratio
1.2e7	1.2e5	8.3	0.15
Anchor rod			
Normal stiffness (kN/m)		Spacing out of plane (m)	
5e5		2.5	
Grout body			
Elastic modulus (kN/m^2)	Diameter (m)	Pile spacing (m)	Skin resistance (kN/m)
7.07e6	0.3	2.5	400

Accepted manuscript doi:
10.1680/jgele.19.00040

Table 3. Effective dissipation time

Benchmark 1	t_e (day)
K_0=1	14
K_0=1.5	25
K_0=2	50

Benchmark 2	t_e (day)
K_0=1	8030
K_0=1.5	10585
K_0=2	19345

Benchmark 3	t_e (day)
K_0=1	18250
K_0=1.5	60225
K_0=2	123370

Table 4. FoS reduction over time

Case	Benchmark 1			Benchmark 2			Benchmark 3		
	K_0=1	K_0=1.5	K_0=2	K_0=1	K_0=1.5	K_0=2	K_0=1	K_0=1.5	K_0=2
Total reduction (%)	8.57	12.15	15.97	10.65	17.64	20.22	13.03	22.66	24.26
Reduction during $t/t_e \leq 0.3$ (%)	8.24	11.37	14.6	10	16.37	17.17	12.65	21.92	22.8
Reduction during $t/t_e > 0.3$ (%)	0.33	0.78	1.37	0.65	1.27	3.05	0.38	0.74	1.46

Accepted manuscript doi:
10.1680/jgele.19.00040

Figure captions

Accepted manuscript doi:
10.1680/jgele.19.00040

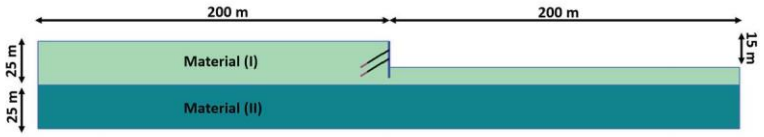

Fig. 1.tif

Accepted manuscript doi:
10.1680/jgele.19.00040

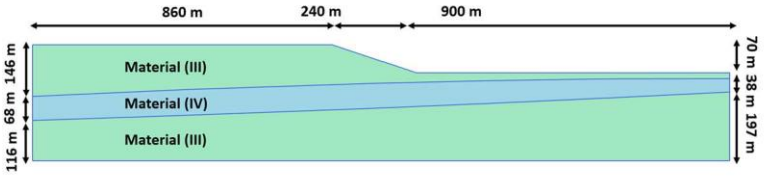

Fig. 2.tif

Accepted manuscript doi:
10.1680/jgele.19.00040

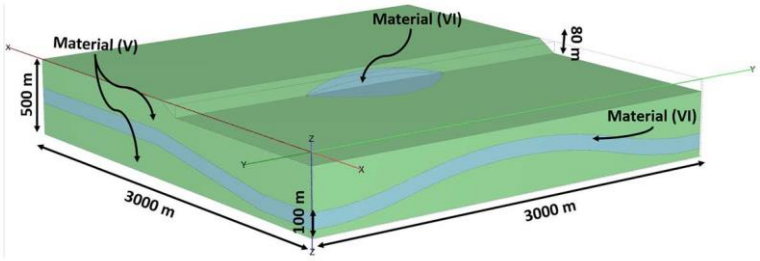

Fig. 3.tif

Accepted manuscript doi:
10.1680/jgele.19.00040

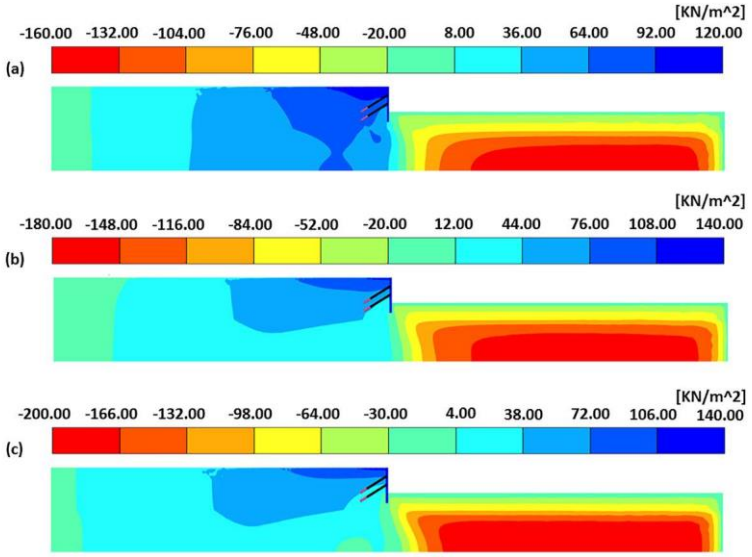

Fig. 4.tif

Accepted manuscript doi:
10.1680/jgele.19.00040

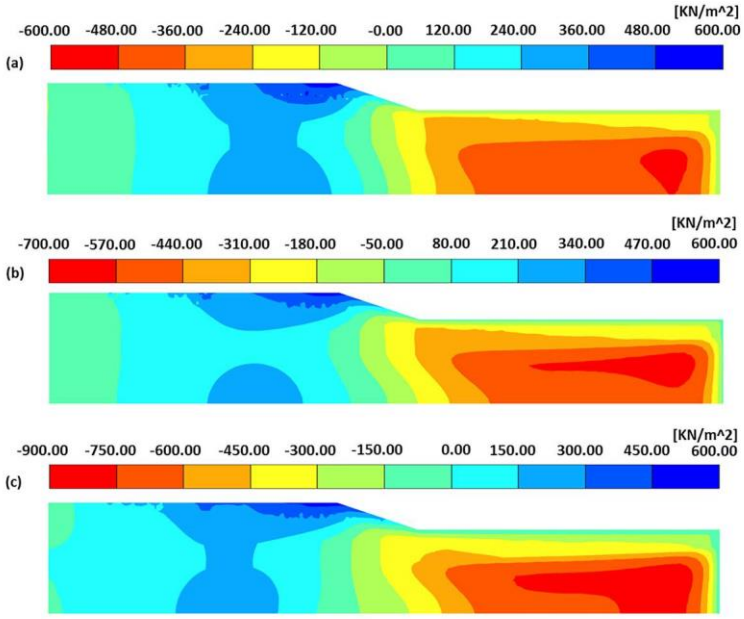

Fig. 5.tif

Accepted manuscript doi:
10.1680/jgele.19.00040

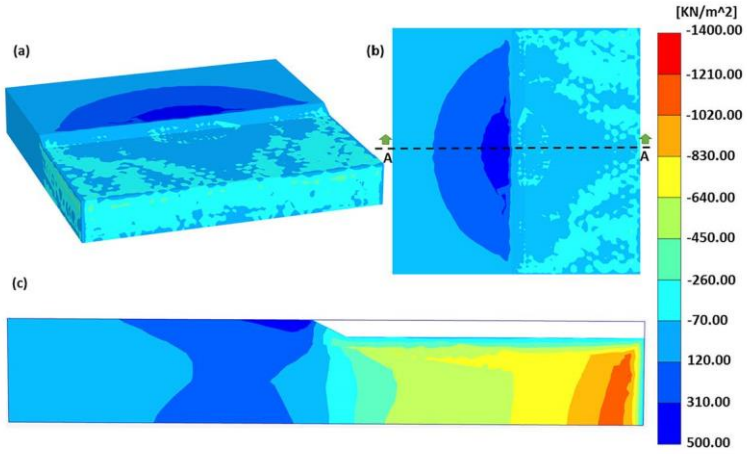

Fig. 6.tif

Accepted manuscript doi:
10.1680/jgele.19.00040

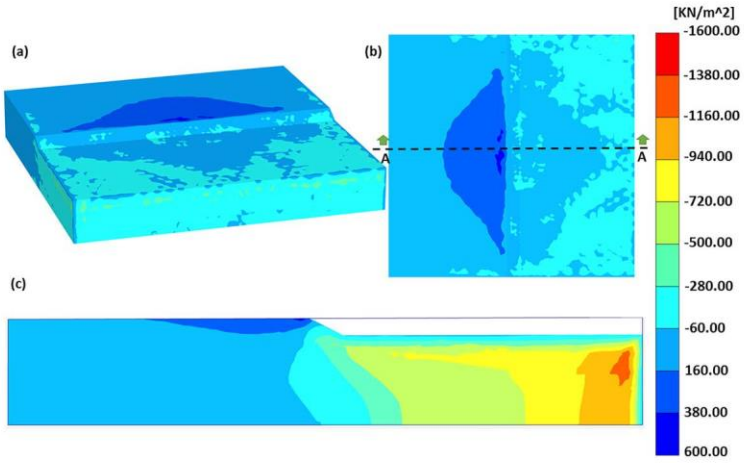

Fig. 7.tif

Accepted manuscript doi:
10.1680/jgele.19.00040

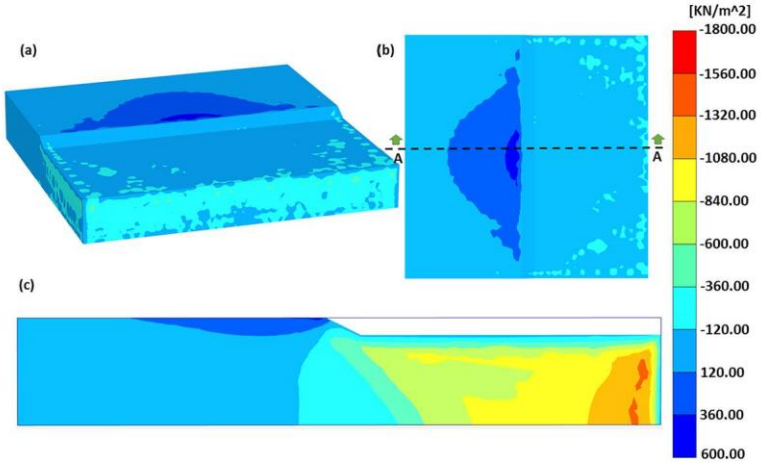

Fig. 8.tif

Accepted manuscript doi:
10.1680/jgele.19.00040

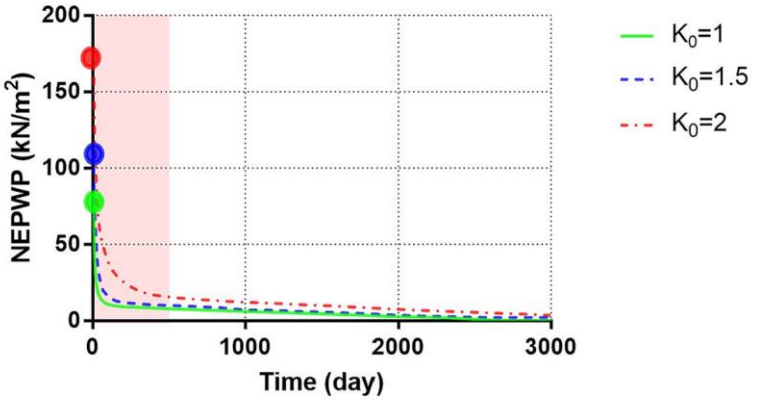

Fig. 9.tif

Accepted manuscript doi:
10.1680/jgele.19.00040

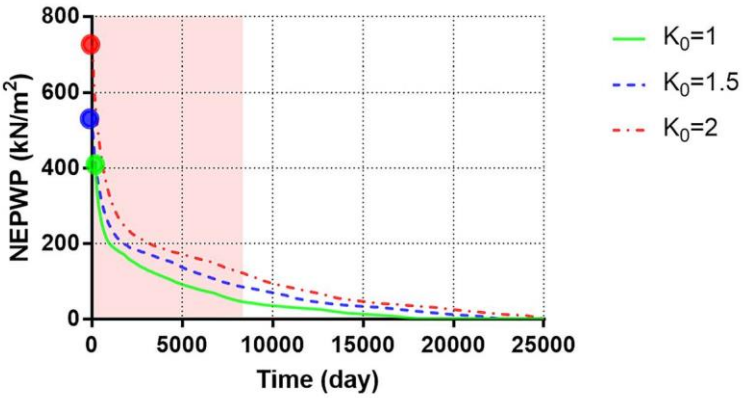

Fig. 10.tif

Accepted manuscript doi:
10.1680/jgele.19.00040

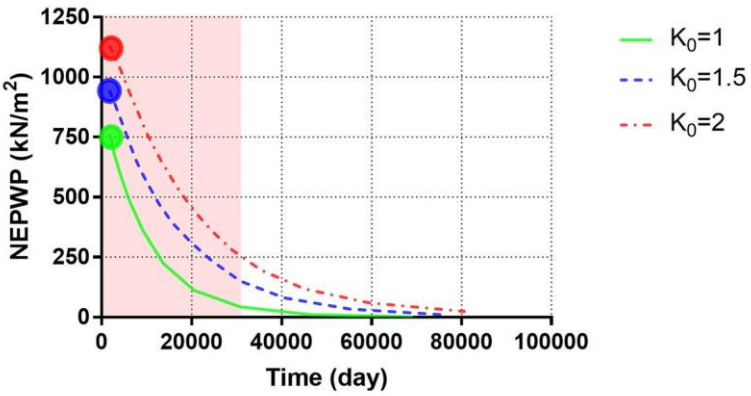

Fig. 11.tif

Accepted manuscript doi:
10.1680/jgele.19.00040

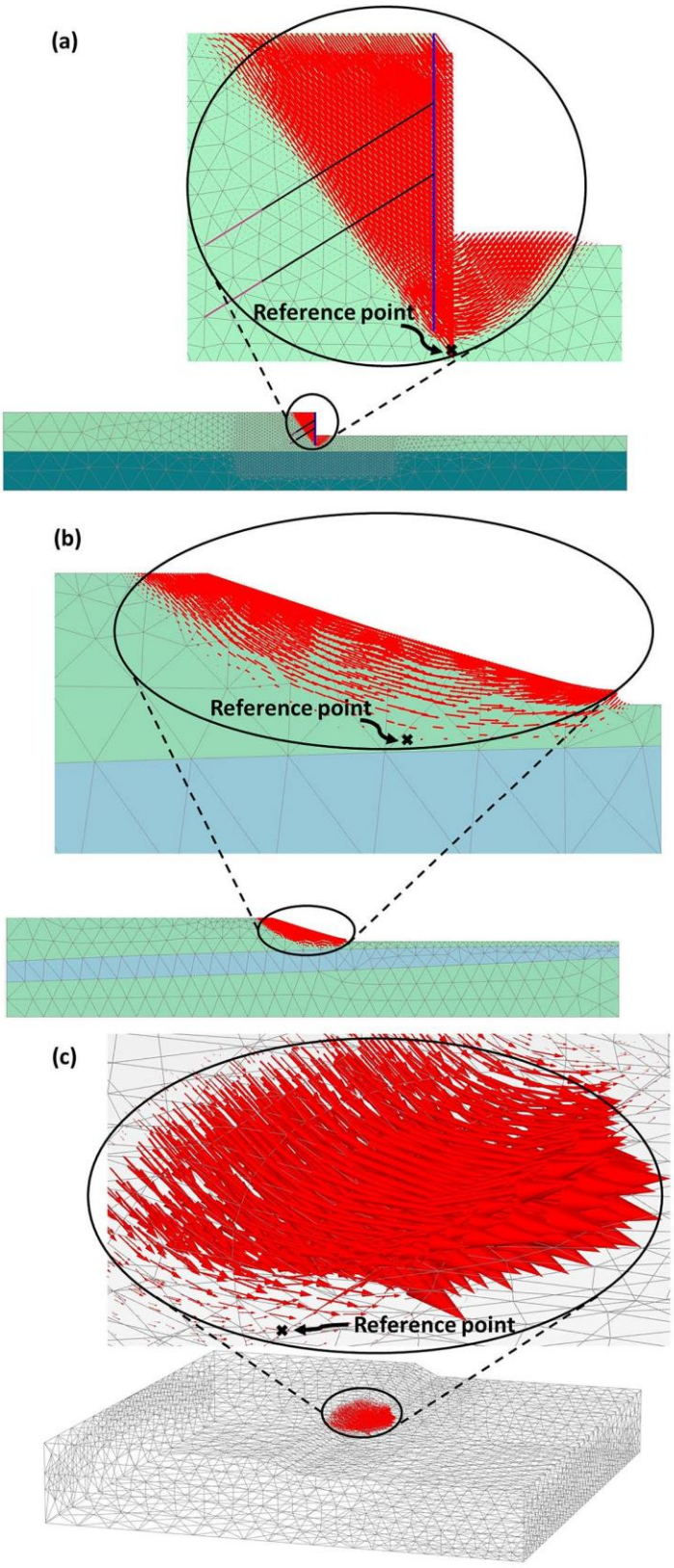

Fig. 12.tif

Accepted manuscript doi:
10.1680/jgele.19.00040

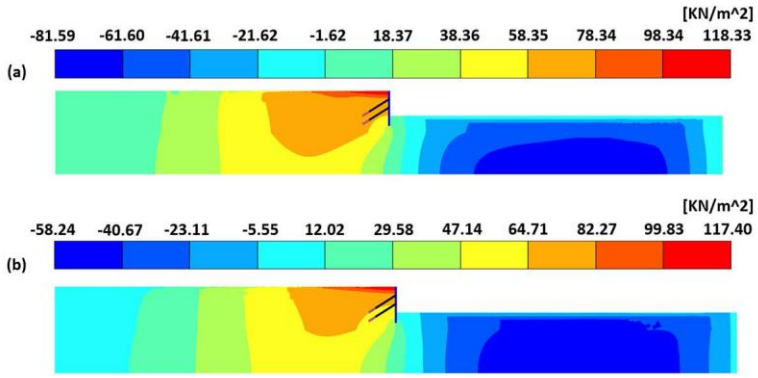

Fig. 13.tif

Accepted manuscript doi:
10.1680/jgele.19.00040

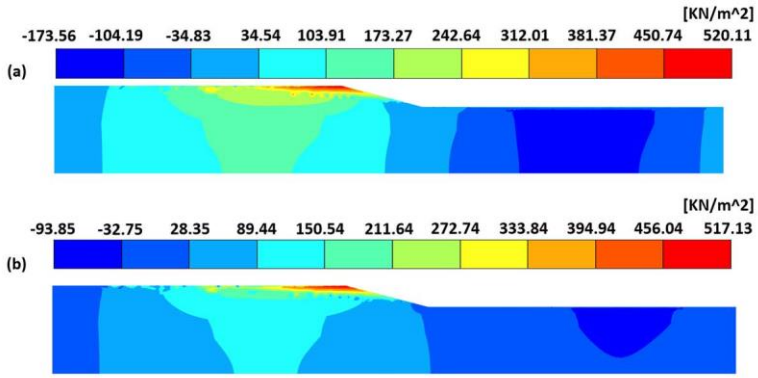

Fig. 14.tif

Accepted manuscript doi:
10.1680/jgele.19.00040

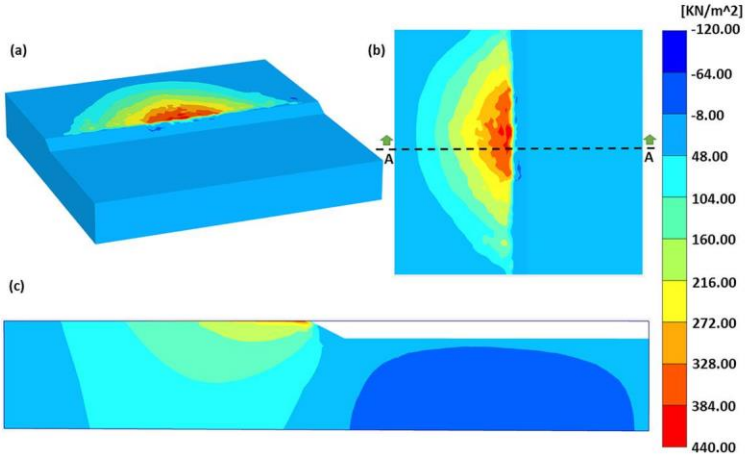

Fig. 15.tif

Accepted manuscript doi:
10.1680/jgele.19.00040

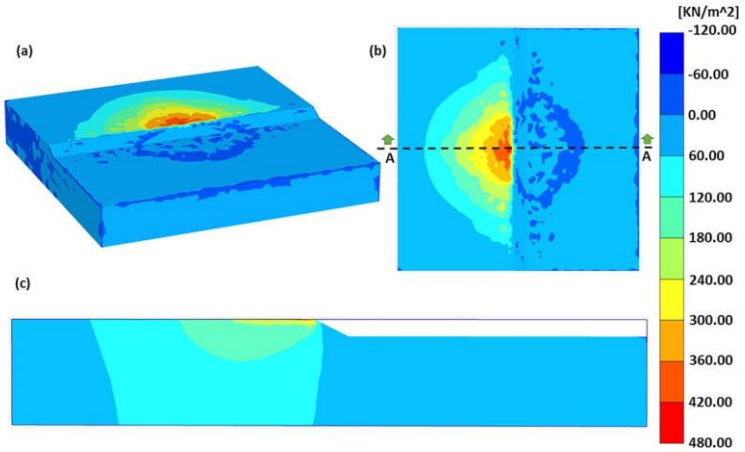

Fig. 16.tif

Accepted manuscript doi:
10.1680/jgele.19.00040

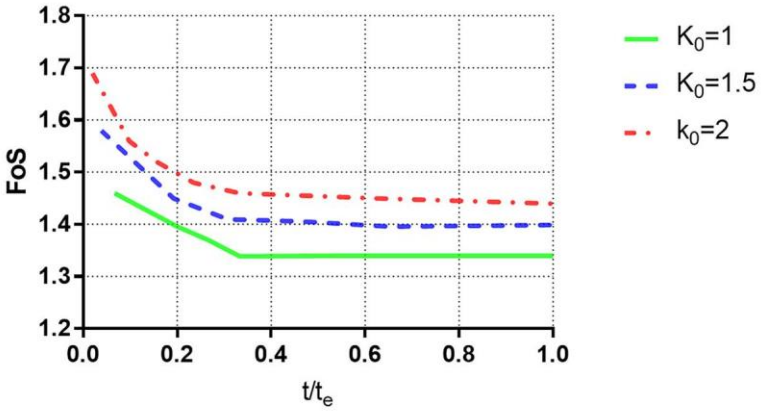

Fig. 17.tif

Accepted manuscript doi:
10.1680/jgele.19.00040

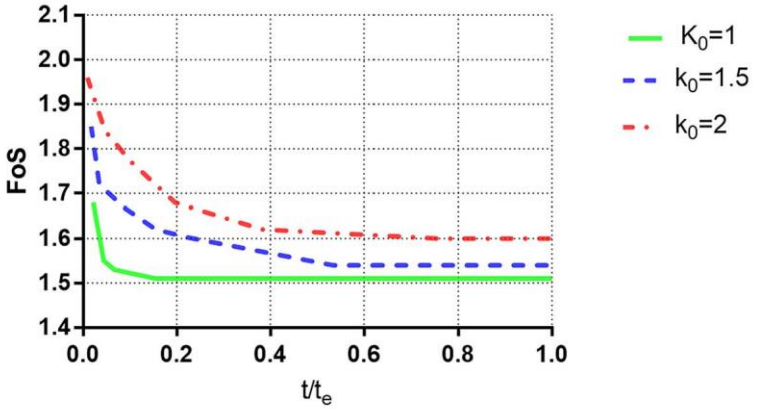

Fig. 18.tif

Accepted manuscript doi:
10.1680/jgele.19.00040

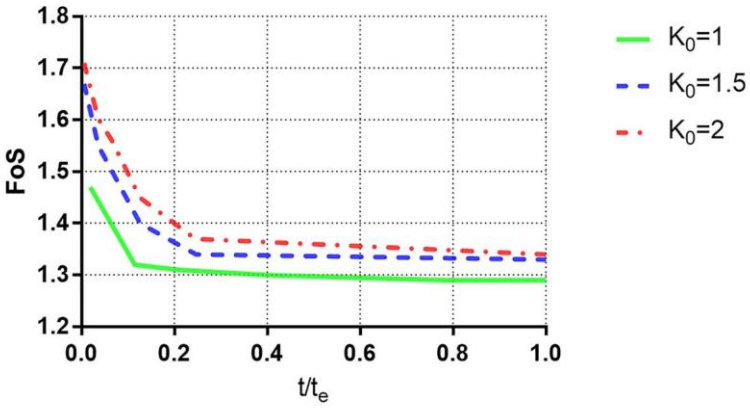

Fig. 19.tif